

This item is the archived peer-reviewed author-version of:

The role of vegetation in the Okavango Delta silica sink

Reference:

Struyf Eric, Mosimane Keotshephile, van Pelt Dimitri, Meire Patrick, Schoelynck Jonas, et al..- *The role of vegetation in the Okavango Delta silica sink*

Wetlands: journal of the Society of Wetland Scientists / Society of Wetland Scientists [McLean, Va] - ISSN 0277-5212 - 35:1(2015), p. 171-181

DOI: <http://dx.doi.org/doi:10.1007/s13157-014-0607-1>

1 The role of vegetation in the Okavango Delta silica sink

2 Eric Struyf¹, Keotshephile Mosimane², Dimitri Van Pelt¹, Mike Murray-Hudson², Patrick Meire¹,
3 Patrick Frings³, Piotr Wolski², Jörg Schaller⁴, Managaliso Gondwé², Jonas Schoelynck¹ & Daniel J.
4 Conley³

5

6 1 University of Antwerp, Department of Biology, Ecosystem Management. Universiteitsplein
7 1C, 2610 Wilrijk, Belgium

8 2 University of Botswana, Okavango Research Institute, Private Bag 285, Maun, Botswana

9 3 Lund University, Department of Geology, Sölvegatan 12, 22362 Lund, Sweden

10 4 Technische Universität Dresden, Institute of General Ecology and Environmental
11 Protection, 01062 Dresden, Germany

12

13 Corresponding author: eric.struyf@uantwerpen.be

14

15 Keywords: tropical wetlands, biogenic silica, Okavango Delta, hydrology

16

17 Abstract

18 We assessed the role of vegetation and hydrology in the Si cycle in the Okavango Delta. Our results
19 show a large storage of biogenic Si (BSi) in vegetation and the sediments. The biological storage is
20 among the highest observed so far for any ecosystem worldwide. Floodplain vegetation accumulates
21 similar amounts of BSi in both the temporary floodplains and the permanent floodplains, with most
22 values observed between 20-100 g Si m⁻². This vegetation Si, after litterfall, contributes to a large
23 biogenic Si storage in the sediments. In temporary floodplains, sediments contain less BSi (375 -1950
24 g Si m⁻² in the top 5 cm) than in the permanent floodplains (1950 - 3600 g Si m⁻² in the top 5 cm). BSi
25 concentrations in the floodplain sediments decline exponentially indicating rapid dissolution. In the
26 occasional and seasonal floodplains, unidirectional solute transfer from floodplains to the islands will
27 remove Si from the riverine systems. Our work clearly emphasizes the crucial role of floodplains and
28 wetlands in Si transport through tropical rivers, and the potential interference of hydrology with this
29 role.

30 Introduction

31 Research on Si cycling in continental ecosystems has received increasing attention in the past
32 decade. While it is clear that large amounts of weathered Si are cycling through ecosystems (Conley
33 2002; Carey and Fulweiler 2012), the quantification of biogenic Si in ecosystem soils and sediments
34 (Barao et al. 2014), how this is related to biogenic Si (BSi) accumulation in vegetation and how this
35 influences Si transport in rivers is still largely enigmatic (Struyf & Conley 2012). Current studies clearly
36 point to the role of wetlands as Si-accumulators in the global biogeochemical Si cycle. Wetlands,
37 situated at the interface between terrestrial and aquatic ecosystems, can act as strong filters on the
38 transport of Si from the continents to the coastal environment (Struyf & Conley 2009), especially
39 because large amounts of Si accumulating grasses often dominate the vegetation. More and more
40 evidence points to the accumulation of Si in wetlands grasses being a functional trait, where uptake
41 of Si is dependent on the environmental stressors experienced by the vegetation, e.g. herbivory or
42 flooding dynamics (Schoelynck et al. 2014; Carey & Fulweiler 2014). As such, wetlands are essential
43 ecosystems to study in the emerging research field of biological control on the continental Si
44 mobilization (Derry et al. 2005). In temperate and subarctic climates, both riparian (e.g. Struyf et al.
45 2009; 2010) and tidal wetlands (e.g. Struyf et al. 2006; Müller et al. 2013) have been studied, but
46 tropical wetlands have not yet received attention.

47

48 The Okavango Delta (Botswana) is one of the world's largest tropical wetland systems, and hence an
49 interesting study area in this regard. It consists of a mosaic of permanent and temporary floodplains,
50 intersected with tree-covered islands (McCarthy et al. 2012). The Okavango Delta's water balance is
51 dominated by evapotranspiration: 98% of all water is lost to the atmosphere before reaching the
52 outlets. The islands play an unusual and essential ecological role in the Okavango Delta as they act as
53 permanent sinks for a major part of the solutes (ca. 360 000 tons a⁻¹) that enter the system (Ramberg
54 & Wolski 2008). Various biological mechanisms result in unidirectional solute transfer from the
55 floodplains to the islands that allow the Delta to remain a productive freshwater wetland ecosystem
56 (Ramberg & Wolski 2008). Evapotranspiration by island trees induces a local lowering of the water
57 table below the islands, creating large hydraulic gradients and inducing lateral groundwater flow. As
58 a result, water infiltrates into the floodplains and flows belowground from the floodplains to the
59 islands bringing dissolved salts with water flow.

60

61 The concentration of dissolved Si (DSi) increases below the islands due to evaporative enrichment,
62 causing precipitation of base-cation rich clays, carbonates and amorphous Si (McCarthy et al. 1998).
63 This causes volumetric expansion, which is a key mechanism of island growth. More soluble

64 components reach the center of the islands (e.g. sodium bicarbonate), where they are lost to deeper
65 groundwater via a density fingering process (Bauer et al. 2006, Zimmerman et al. 2006).

66

67 The role of biota in the formation of islands has been recognized. Islands in the Delta initiate around
68 a termite mound, gradually building from this basis (McCarthy et al. 1998). Large trees – which are
69 especially dense on the island fringes (McCarthy et al 2012) - play an essential role in maintaining the
70 hydraulic pressure gradient through transpiration. However, while the role of islands in sequestering
71 Si is known, we have little understanding of the role of vegetation in depositing and sequestering Si
72 in the floodplains, though they actually cover a much greater surface area. We here hypothesize that
73 floodplain vegetation plays an essential role in the assimilation of dissolved Si from the water and,
74 after dissolution of plant material, its delivery to the island sub surfaces. The selective removal of
75 dissolved Si from the Okavango Delta surface waters has been identified, based on its relative
76 enrichment in concentration below that expected from evaporation and rain water input (Sawula &
77 Martins 1991). However, Si precipitation has not been linked earlier to floodplain vegetation
78 associated processes.

79

80 Vegetation in the Okavango Delta floodplains mainly consists of sedges and grasses, with key species
81 including *Miscanthus junceus*, *Cyperus papyrus* and *Phragmites australis*. These species are well
82 known Si accumulators, with elemental Si concentrations in *P. australis* reaching 5% of dry biomass
83 (e.g. Struyf et al. 2007). Si in vegetation occurs as BSi mainly in structures called phytoliths, deposited
84 at sites of transpiration. Plant BSi plays a role in stress resistance and intra/interspecific competition,
85 e.g. increasing resistance against flow shear stress and salt stress (e.g. Cooke & Leishman 2011). In
86 aquatic macrophytes, BSi has a role similar to lignin and cellulose, increasing the capability of
87 vegetation to withstand high flows and to maintain an upright stature, important for sustained
88 photosynthesis in flooded environments (Schoelynck et al. 2010). Apart from vegetation, diatoms are
89 also prominent in the Delta floodplains (e.g. Mackay et al. 2012; Davidson et al. 2012) and have an
90 obligate requirement for dissolved Si for building their frustules. Thus, there is a large potential for
91 biologically mediated Si accumulation in the floodplains of the Okavango Delta, corroborated by
92 previous research which suggests the substantial occurrence of plant phytoliths in the peat of the
93 permanent floodplains (McCarthy et al. 1989).

94

95 We hypothesize that biogenic Si accumulation in the vegetation functions as a trapping mechanism
96 for most of the DSi entering and flowing through the Delta. After vegetation senescence, the BSi
97 contributes to the accumulation of biogenic Si in floodplain sediments, where it is available for
98 dissolution. After dissolution, DSi may be taken up again by the vegetation or transported further

99 down the Delta. Crucially, a significant part may also be transported along with lateral water flow to
100 the island sub-surfaces.

101

102 We sampled the uppermost sediments on both islands and floodplains and the associated
103 vegetation, along gradients from island centers to the channels bordering the floodplains at both a
104 temporary and a permanent floodplain and their adjacent islands. We make conservative estimates
105 of the storage of BSi in the vegetation and compare it to annual inputs of Si into the Delta, then
106 relate this to Si storage patterns across hydrological gradients within floodplain sediments. We
107 hypothesize that the highest storage of biogenic Si in the sediments will occur in areas with
108 permanent inundation, while the highest dissolution potential of accumulated BSi exists in the
109 temporal floodplains, where strong hydraulic pressure from floodplains to islands causes more
110 frequent water refreshing, enhancing porewater leaching of DSi (recycled from BSi).

111

112 Study site and transect sampling

113 The Okavango Delta (Fig. 1) is in fact not a delta but a low gradient (1:3400) alluvial fan (McCarthy et
114 al. 1998). The inundated area of the Delta fluctuates from 6,000 km² during low flow seasons to over
115 15,000 km² during high flow seasons (Gumbricht et al 2004). The annual flood pulse that inundates
116 the Okavango Delta originates as precipitation in the highlands of Angola and reaches the Mohembo
117 inlet (Botswana) by February through June, peaking in April. The mean annual discharge into the
118 Delta is approximately $9.0 \times 10^9 \text{ m}^3$ (McCarthy et al., 2003). It takes about four months for the flood
119 water to reach the most downstream distal reaches of the Delta near Maun, Botswana about 260 km
120 from the inlet at Mohembo (Wolski et al. 2006). Direct rainfall into the Delta contributes about 42 %
121 (about $6 \times 10^9 \text{ m}^3$ per annum) to the mean flow, mostly by summer rains out of phase with the
122 riverine flood-pulse (Ramberg and Wolski, 2008). The Okavango Delta annually receives between
123 0.0024 and 0.0036 TMol ($\times 10^{12}$ mol) of DSi from the Okavango River which flows into the Delta
124 through a narrow conduit called the Panhandle (Ramberg & Wolski 2008, calculated using water
125 input and measured Si concentrations in the Panhandle).

126

127 The Okavango Delta has been divided into physiographic regions: (i) the Panhandle, the confined
128 entry channel; (ii) the permanent swamp; (iii) the seasonal and occasional swamps. The Okavango
129 River (~100 m width) flows into the Panhandle (~25km wide) where it meanders through a
130 permanently-flooded *Cyperus papyrus* dominated landscape. From the Panhandle the Okavango
131 River enters the permanent swamps where it divides into three main distributary channels. The
132 permanent swamp is intersected by channels, lagoons and lakes, dominated by emergent *C. papyrus*.
133 Water movement in the permanent swamps is slow due to the low gradient and the submerged and
134 emergent vegetation, and dry land surfaces are relatively small. The seasonal swamp and occasional
135 swamps (hereafter referred to as temporary swamps) have more prominent dry land areas. In the
136 temporary swamp, flood waters flow mainly through channels, bordered by grasses and reeds, and
137 overflow onto shallow, grassy floodplains. Most islands are thus found in the temporary floodplains
138 in the distal ends of the delta, where they cover over 50% of the total surface area. The exact
139 proportion is variable and depends on the actual extent of the flooding (Gumbricht et al. 2004).

140

141 Subsurface geology of the 165,000 km² catchment is dominated by Precambrian/Palaeozoic
142 continental cratons and is nearly entirely overlain by highly weathered Kalahari sands of Cenozoic
143 age, in places >300 m deep, whose influence dominates the Okavango River dissolved and suspended
144 loads. Clay mineral neoformation occurs throughout the Delta – when the geochemistry permits

145 (Frings et al. 2014): however, the majority of element sequestration occurs beneath the islands
146 (Frings et al. 2014).

147

148 We selected two island-floodplain gradients in the Okavango Delta: one in the permanently flooded
149 wetlands (“Guma”) and one in the temporary wetlands (“Nxaraga”) (Fig. 1). At both locations, we
150 sampled sediment and vegetation along full hydrological gradients, from the center of the islands to
151 the edges of the channel bordering floodplain. These gradients were subdivided into 9 (Guma) and
152 12 (Nxaraga) sampling locations respectively, representing the visual variability in vegetation cover
153 (or absence thereof). Vegetation and surface sediment samples (25 cm) were taken at each of these
154 sampling sites, as described below. Additionally, at Nxaraga, deeper (max 8m) boreholes were drilled
155 in 5 island sampling sites and one floodplain sampling site.

156

157 Materials and methods

158 Sampling

159 Aboveground vegetation and litter samples were taken from two random quadrats (0.25 m²) at each
160 selected sampling site (no trees were sampled, only herbaceous/grass vegetation and litter).
161 Standing biomass is at its peak at the time of sampling. Vegetation species composition was
162 determined during cutting (Table 1). At each selected sampling point along the transects, three
163 sediment cores (25 cm length and 28 mm ϕ) were sampled using a hammer auger with a removable
164 plastic lining (Eijkelkamp 04.15.SA Foil sampler). The sediment cores were each subsampled at 6
165 different depths and pooled per depth per sampling spot. The litter layer was included in the
166 vegetation samples and not the sediment core. Depths at which samples were taken were not
167 exactly the same at all sampling spots, as we took into account clearly visible horizons of organic and
168 inorganic sediment. In general, the first 10 cm was sliced into three parts and the next 15 cm also.
169 The samples were wet-weighed, immediately frozen and stored until analysis. Along an overlapping
170 transect at Nxaraga (Fig. 1), six boreholes were drilled by large-diameter hand-auger (Eijkelkamp)
171 along the island-floodplain gradient to a maximum depth of 8m using hole casing and a bailer where
172 necessary. Samples of ~40g were taken every 25cm from the visually undisturbed/uncontaminated
173 centre of the auger, and stored cool in zip-lock bags until freeze-drying.

174

175 Si Analysis

176 Vegetation samples (litter + aboveground vegetation) were thoroughly rinsed and cleaned to remove
177 sediments, epiphytic algae and macro-invertebrates. Subsequently, they were oven dried at 75°C for
178 three days (72 hours). The dried samples were weighed immediately after removing from the oven
179 and then ground and homogenized (< 0.5 mm) in bulk. The total BSi content of the bulk vegetation
180 from every quadrat was analysed: 25 mg biomass was digested with 25 ml 0.094 M Na₂CO₃ for 6
181 hours at 80 °C (e.g. Struyf et al. 2005). For the most abundant species, individuals were selected in
182 the area directly next to the sampling spots, for analysis of BSi in these individual species. Individual
183 species analyses refer to the whole aboveground biomass: no organ-specific extraction was
184 performed.

185

186 Sediment samples were dried using an IMA-Telstar Cryodos-50 freeze dryer, sieved at 500 μ m to
187 remove macroscopic plant and shell material before analysis, and weighed for bulk density.
188 Subsequently, they were digested in 30 ml of 0.094 M Na₂CO₃ in a shaking water bath at 80 °C (e.g.
189 Struyf et al. 2009; 2010). After 4, 5 and 6 hours, subsamples were taken and analyzed with an ICP-
190 OES (iCAP 6300 Duo, © Thermo Scientific) or by the molybdate blue spectrophotometric method (for
191 the borehole samples only) for extracted DSi (all Si concentrations expressed as elemental Si further

192 on, and not SiO_2). To correct for the amount of Si resulting from mineral dissolution, the Si content of
193 the subsamples was plotted against dissolution time. All biogenic Si dissolves within the first few
194 hours: the y-axis intercept of the linear least-squares regression line through the measured values
195 represents the estimated BSi content (DeMaster 1981). Recent research has clearly shown that non-
196 biogenic Si fractions can interfere with the extraction of BSi (Struyf & Conley 2012), e.g. other
197 amorphous Si fractions like adsorbed Si. The term ASi (amorphous Si) has therefore been adopted by
198 other studies. The analysis is currently undergoing rapid methodological development (Barao et al.
199 2014). Recent insights show that extraction using 0.094 M Na_2CO_3 could also lead to an
200 underestimation of the total BSi content, as some fractions of phytoliths only dissolve in stronger
201 alkaline solutions (e.g. 0.5 M NaOH) (e.g. Saccone et al. 2007; Meunier et al. 2014). However, these
202 stronger solutions also more readily extract mineral silicates. Due to the abundance of quartz and
203 kaolinite in Okavango sediments (e.g. McCarthy et al. 1989), we used 0.094 M Na_2CO_3 . This also
204 facilitates comparison to most other studies on soil BSi storage, which have typically applied Na_2CO_3
205 to digest BSi (e.g. Clymans et al. 2011; Carey & Fulweiler 2013). In this manuscript, we decide to
206 adopt the term BSi for alkaline extracted Si in both surface sediments and vegetation. In sediment,
207 the mainly biogenic origin of the extracted Si was confirmed by microscopical analyses (Frings et al.
208 2014). However, for the deep cores we adopted the term ASi, as earlier research has confirmed that
209 large non-biogenic amorphous Si precipitates here constitute most of the amorphous Si. Si
210 concentrations in vegetation and litter are expressed as elemental Si per total dry biomass (%).
211 Sediment BSi or ASi (for the deep cores) is expressed as elemental Si relative to the total weight of
212 dry sediment (%). Si stock calculations were calculated from the multiplication of biomass per
213 quadrat and relative BSi content of the biomass. Sediment Si stocks are calculated from the total
214 sediment weight on a square meter basis, for either 5 or 25 cm depth, based on the bulk density, and
215 the relative elemental BSi (or ASi) content of the sediment.

216

217

218 Results

219

220 Vegetation BSi

221 Vegetation samples included only herbaceous vegetation, grass and leaf litter, and only leaf litter at
222 the forest site (GumDr5). The dominant species cover at each sample site is shown in Table 1.
223 Vegetation generally contained a higher stock of BSi in the Guma floodplain compared to the Guma
224 island (except for the riparian forest site). At Guma, floodplain vegetation contained between 20 and
225 80 g BSi m⁻², while island vegetation contained between 1 and 30 g m⁻². The tendency for lower
226 vegetation BSi stock on the island was also clear in Nxaraga (2 – 40 g m⁻²), whereas floodplains
227 contained about 20-160 g BSi m⁻² in the vegetation (Fig. 2). Vegetation BSi concentrations at islands
228 and floodplains showed no clear island/floodplain distinction. At Guma, island vegetation contained
229 (for complete sampled plots) on average 1.7% of BSi (range 1.2% - 2.8%) and floodplain vegetation
230 contained 2.5% BSi on average (range 1.0% - 3.4%). At Nxaraga, island vegetation contained (for
231 complete sampled plots) on average 2.3% of BSi (range 1.6% - 2.6%) and floodplain vegetation
232 contained 1.9% BSi on average (range 0.9% - 2.9%). Differences in stocks were fully attributable to
233 the high biomasses occurring in the floodplains.

234

235 Sediment BSi

236 *Permanent floodplains (Guma)*

237 At the Guma site, BSi in the island sediment was both low in concentration (Fig. 3) and in total stock
238 (Fig. 2). In the driest parts of the island, sediment BSi concentrations were between 0 and 0.5%. In
239 the riparian forest (GumDr5), sediment BSi concentrations were slightly higher than at the other
240 island sites (Fig. 3). In the permanent floodplains, BSi exhibited different behaviour. Surface BSi
241 concentrations ranged between 1 and 5% BSi, then gradually decreased with depth to <0.5% in all
242 cores (Fig. 3). Stocks of BSi in the permanent floodplains (top 5 cm) were between 100 and 550 g BSi
243 m⁻² at sites on the islands, and between 1950 and 3600 g m⁻² in the floodplains themselves (Fig. 2).
244 Storage over the full 25 cm depth ranged between 1300 and 4600 g BSi m⁻² on Guma island and
245 between 5200 and 10500 g BSi m⁻² in the Guma floodplains.

246

247 *Temporary floodplains (Nxaraga)*

248 At the driest island sites in the temporary floodplain region, BSi concentrations were low throughout
249 the cores and generally below 0.5% BSi (Fig. 3). At the two riparian forest sites (NXADr4 and NXADr5),
250 concentrations were higher averaging 1% with slightly higher values in the deeper section (20-25
251 cm). Overall, variability in BSi from the island cores was low. In the Nxaraga floodplain cores, BSi

252 concentration decreased with depth in the 5 cores closest to the channel. Maximum concentrations
253 at the surface between 0.6 and 1.7% BSi was always lower than in the permanent floodplains at
254 Guma (Fig. 3). In the two floodplain cores closest to the island, surface BSi concentrations were
255 always 0.4% BSi or lower. In all floodplain cores, BSi concentrations at depth (20-25 cm) were lower
256 than 0.4%. BSi stocks in the top 5 cm of sediment were similar across the entire transect in cores
257 from Nxaraga island and its floodplains, ranging between 175 – 1300 g m⁻² (island cores) and 375-
258 1950 g m⁻² (floodplain cores). This is in stark contrast to the clear separation between floodplains and
259 islands in the permanently flooded transect at Guma (Fig. 2). BSi stocks (25 cm profile) ranged
260 between 800 and 7200 g m⁻² in Nxaraga island and between 1300 and 3900 g m⁻² in the floodplain
261 with the highest BSi accumulation in the riparian forest sites on the island.

262 ASi concentrations at Nxaraga were also explored further in deep cores up to 8m depth (Fig. 4). The
263 floodplain coring here clearly shows that negligible concentrations of ASi (<0.3 %) occur through the
264 deeper layers up to 8 m depth. In the island cores, a clear accumulation peak of ASi can be observed
265 at about 3-3.5 meters in the centre of the island and the riparian forest, with concentrations up to
266 4.5%. Concentrations in the other island cores generally ranged between 0.5 and 2% throughout the
267 depth profile.

268

269

270 Discussion

271

272 Our results indicate that in the Okavango Delta, the trapping of DSi by vegetation is an important
273 step in the retention of Si. Floodplain vegetation stores similar amounts of BSi in both the temporary
274 floodplains and the permanent floodplains, with most values observed between 20-100 g Si m⁻². For
275 sediment BSi storage, most of the BSi occurs in the upper layers. The temporary floodplains (375 -
276 1950 g BSi m⁻² in the top 5 cm) contain less BSi than the permanent floodplains (1950 - 3600 g BSi m⁻²
277 in the top 5 cm). BSi concentrations in the floodplain sediment decline exponentially indicating rapid
278 dissolution of BSi with most dissolution occurring within the first 5 cm. The top sediment layers
279 represent a reservoir of biologically accumulated Si that rapidly recycles.

280

281 Sediment accumulation rates in the Okavango Delta can reach up to 5 cm per year in certain settings
282 (McCarthy et al. 1989). If we assume a recent estimate of ~0.25 cm a⁻¹ is more representative of
283 average accumulation (Bernal and Mitsch 2013), this implies between 100 and 175 g of BSi is
284 recycled annually to DSi per m² in the top 5 cm in the permanent floodplain, based on the decrease in
285 BSi concentrations in the sediment. Rapid rates of recycling from marsh grass litter have been shown
286 in tidal wetlands and under experimental conditions (Struyf et al. 2007; Schaller & Struyf 2013), but
287 are unavailable currently for tropical wetlands. Future studies on dissolution rates of Si from tropical
288 wetland litter are necessary to quantify recycling rates in more detail. Most of the “recycled” DSi will
289 end up in the vegetation again, as annual biomass production is approximately double the standing
290 vegetation stock in the permanent floodplains (McCarthy et al. 1989), requiring annual uptake of 40-
291 200 g DSi m⁻² a⁻¹. Spatially distributed riverine annual input from the Okavango river is ca. 20 g m⁻² in
292 the permanent floodplains (assuming 6000 km² of permanent floodplain and an annual input of
293 0.0030 Tmole of Si). Our calculations require efficient recycling to support the majority of BSi
294 production. Some fraction of the dissolved BSi will not be taken up again by vegetation, and will be
295 exported as DSi from the floodplain sediment, either infiltrating deeper into the sediment or
296 transported further downstream into the Delta. This can be replenished by the spatially distributed
297 annual riverine input into the permanent floodplain.

298

299 In the temporary floodplains, abundant islands create a larger hydraulic head between surface water
300 and island groundwater. This probably is an important cause for both lower BSi concentrations and
301 stocks in the temporary floodplain relative to the permanent floodplain. Despite approximately
302 equal amounts of BSi in vegetation in the two regions, the lowest values for sediment BSi storage in
303 the permanent floodplains were greater than the highest values in the seasonal floodplains. In
304 contrast to the permanent floodplains, a strong unidirectional transport of water from floodplains to

305 island interiors is present in the temporary inundated areas. Given the large surface area of islands in
306 the temporary floodplains, the vast majority of Si accumulated is in the interior of the islands, in
307 contrast to the permanent floodplain where island surface area is limited (Gumbrecht et al. 2004).
308 This is confirmed in the ASi data in deep cores. It is not surprising that the islands only accumulate
309 small amounts of ASi in the top layers: most Si accumulates underneath the islands in the deeper
310 sediment horizons, especially below the riparian forest. Earlier and our data show the greatest
311 accumulation of Si and other elements in the islands at the sites of strongest evapotranspiration, i.e.
312 the forested island fringes (Bauer et al 2004). The importance of amorphous Si precipitates in the
313 build-up of islands has been pointed to in earlier research (e.g. Ramberg & Wolski 2008; McCarthy et
314 al. 2012).

315

316 Tropical wetlands and Si cycling

317 Our results clearly show a large surficial storage of biogenic Si in the Okavango Delta. We used
318 estimates of the areas of islands, permanent and temporary floodplains from Gumbrecht et al. (2004)
319 to assess total storage of BSi in the top 25cm only of the Okavango Delta sediment, not taking into
320 account deeper storage. Taking the lowest BSi storage amounts observed for the different delta
321 sections, we can conservatively estimate total surficial BSi storage of 0.4 Tmole of Si in the
322 permanent floodplains, 0.2 Tmole in the temporary floodplains and 0.01 Tmole in the islands, leading
323 to a minimum estimate of 0.6 Tmole of BSi storage in the Delta. Alternatively, taking the upper-end
324 estimates of our data results in storage values of 0.8 Tmole, 0.4 Tmole and 0.07 Tmole respectively,
325 implying total Delta storage of 1.3 Tmole of Si in the top 25 cm. This surface storage represents about
326 200-400 years of DSi input into the Delta, as annual (modern day) input equals ~ 0.003 Tmole. Based
327 on a vegetation BSi turnover (see earlier) of $100 \text{ g Si m}^{-2} \text{ a}^{-1}$, vegetation uptake in the floodplains
328 represent about $0.020 \text{ Tmole a}^{-1}$, compared to an annual input of $0.003 \text{ Tmole of Si}$ into the Delta.

329

330 The BSi storage in both the permanent and temporary floodplains is among the highest observed so
331 far for any ecosystem worldwide (Struyf & Conley 2012), at $110\text{-}220 \times 10^3 \text{ kg SiO}_2 \text{ ha}^{-1}$ and $42\text{-}80 \times 10^3$
332 $\text{kg SiO}_2 \text{ ha}^{-1}$ respectively. This exceeds the highest values published to date, where BSi pools over a
333 full soil profile of between 30 and $104 \times 10^3 \text{ kg SiO}_2 \text{ ha}^{-1}$ were observed in soils from the Great Plains
334 grasslands and equatorial rain forests (Blecker et al. 2006; Alexandre et al. 1997). The floodplains of
335 the Okavango Delta also greatly exceed values observed in temperate tidal marshes and subarctic
336 peat bogs (between $12\text{-}32 \times 10^3 \text{ kg SiO}_2 \text{ ha}^{-1}$) (Struyf et al. 2005; 2010). It should be emphasised that
337 our estimates are conservative, particularly since we used a weak base extraction ($0.094 \text{ M Na}_2\text{CO}_3$)
338 and we are only integrating the top 25 cm of the sediment horizon whereas the other estimates are
339 typically based on 1-2 m horizons. Some aged phytolith material as well as sponges may not have

340 completely dissolved after only a few hours in 0.094 M Na₂CO₃ (Meunier et al. 2014). However, given
341 the rapid recycling of BSi in sediments, we assume that aged diagenetically altered phytoliths are
342 unlikely to represent a major fraction of BSi in our sediments. Part of the BSi we analysed likely
343 derives from sponges (unpub. data), base-cation rich clays, reactive secondary silicate minerals and
344 from non-biogenic amorphous reactive Si phases, including Si adsorbed to aluminum- or iron oxy-
345 hydroxides (McKeague and Cline 1963). Fractionation between these non-biogenic and biogenic Si
346 phases should be a research priority in the future.

347

348 Recently, Carey & Fulweiler (2013) estimated annual, BSi uptake in global vegetation of about 85
349 Tmole. Of this, they calculated that the total surface of wetlands worldwide contributes
350 approximately 4.16 Tmole a⁻¹. Our conservative vegetation BSi production estimate of 0.02 Tmole of
351 Si a⁻¹ would represent about 0.4% of total annual uptake in wetland vegetation worldwide within the
352 Okavango Delta alone, despite it covering only about 0.1% of global wetland area (Mitsch et al.
353 2013). Although data for other tropical wetlands are limited, Cary et al. (2005) observed 2-4 % of BSi
354 in swamp soils in the Nyong river basin in Cameroon, in the same range as concentrations in the
355 Okavango. Tropical rivers deliver about 70-80% of the global DSi load into the ocean (Jennerjahn et
356 al. 2006), implying it is crucial to assess environmental factors that can influence its transport. Our
357 data and the limited available literature data available clearly show that wetlands and floodplains are
358 an important yet understudied component. Other studies have indicated the potential influence of Si
359 uptake by giant grasses and sedges (e.g. Ding et al. 2008) through Si-isotope biogeochemistry in
360 tropical rivers.

361

362 The hydrology of many tropical wetlands is undergoing major changes due to human alteration of
363 river morphology and watersheds. Model predictions also project substantial future changes in
364 hydrology and climate (Hamilton 2010; Wolski et al. 2014). This will have implications for flooding
365 extent and seasonality, factors that may induce changes in Si storage in the Okavango Delta. While
366 vegetation is an important trap for Si in the permanently inundated wetlands, permanent long-term
367 burial in sediments is likely low, as indicated by near-negligible BSi concentrations in the deeper
368 layers. These conditions imply that reactive Si stores in the permanent floodplains are still intimately
369 connected to flooding water, and thus a significant part of recycled Si is leaching back into “river”
370 water after BSi dissolution. However, in the occasional and seasonal floodplains, unidirectional solute
371 transfer from floodplains to the islands will remove reactive Si from the riverine systems (Figure 5).

372

373 Outlook

374 Our results show that wetland vegetation in the Okavango Delta plays a key role in the annual Si
375 budget of the Okavango Delta. Most of the DSi entering the permanent floodplains cycles through
376 vegetation before transport further downstream. There is a clear distinction in the amount of BSi
377 sequestered between permanent and temporary floodplains. While BSi stores are actively recycled in
378 the sediments of the permanent floodplains (implying strong potential for leaching to surface
379 waters), unidirectional transport of Si leads to the loss of recycled BSi into the tree covered islands in
380 the temporary floodplains. Our work clearly emphasizes the crucial role of floodplains and wetlands
381 in Si transport through tropical rivers.

382

383 Although our results are conservative estimates, our analysis indicates that the sediments of the
384 Okavango Delta represent the largest store of sediment or soil BSi per m^{-2} yet identified worldwide.
385 This emphasizes the necessity to construct an estimate of worldwide BSi storage and accretion or
386 depletion rates in soils and sediments, which has still only been quantified in a limited number of
387 ecosystems and with a restricted global distribution of sites studied (Struyf & Conley 2012), and to
388 initiate studies on how the storage is affected by environmental conditions, e.g. flooding frequency,
389 sediment and porewater pH and salinity in wetlands. Future studies in wetlands should also
390 investigate the exact nature of stored Si through microscopical studies, and better constrain
391 dissolution/retention fluxes through e.g. the detailed study of porewater profiles and potentially
392 isotope fractionation. A recent study by Frings et al. (2014) shows this potentially provides added
393 insight on processing of the large stocks of Si present in the Okavango delta, and wetlands in general.
394 This will further allow a more nuanced understanding of whether the global Si cycle operates in
395 steady state, or is instead characterised by time-lagged responses to anthropogenic or natural
396 changes (Frings et al. 2014).

397

398 Based on high rates of vegetation accumulation we observed in the Okavango, the most recent
399 estimate of annual uptake of vegetation BSi production (Carey & Fulweiler 2013) of $\sim 84 \text{ Tmole Si}$
400 year^{-1} could be underestimated. In our dataset, storage in floodplain sediments is 45 times greater
401 than annual vegetation uptake. In *Phragmites australis* dominated tidal temperate wetlands, where
402 daily tidal immersion/emersion cycles induce strong recycling potential, the uptake/storage ratio was
403 about 40 (Struyf et al. 2005), while for bamboo, deciduous and coniferous forests with perennial
404 vegetation, ratios of over 1000 are proposed (Conley 2002). This represents massive soil storage
405 relative to annual continental Si fluxes ($7.2 \text{ Tmole Si a}^{-1}$; Tréguer & De La Rocha 2013) and annual
406 weathering fluxes ($10\text{-}40 \text{ Tmole Si a}^{-1}$, Hilley & Porder 2008), showing the clear need for a better
407 quantification of sediment BSi accumulation rates.

408 Acknowledgements

409 We would like to thank several funding agencies for their funding contributions: University of
410 Botswana, EU Marie Curie Program (Hobits), National Geographic Explorer Grant, the Swedish
411 National Science Foundation (VR) and the Knut and Alice Wallenberg Foundation. We would like to
412 thank BELSPO for funding the project SOGLO.

413 Table 1

414 Dominant vegetation (all species with higher than 5% cover in the plot) summarized for all
 415 the sampling spots. In the site column, the first three letters refer to the sampling location
 416 (Nxa : Nxaraga, Gum : Guma). “Dr” and “Wet” refer to respectively islands and floodplain
 417 sites.

site	total cover	Dominant species
NxaDr1	20	<i>Sporobolus spicatus</i> (20%)
NxaDr2	25	<i>Cynadon dactylon</i> (15%), <i>Schoenoplectus corymbosus</i> (5%), <i>Cyperus longus</i> (5%)
NxaDr2	80	<i>Eragrostis lappula</i> (75%), <i>Cynadon dactylon</i> (5%)
NxaDr2	85	<i>Panicum repens</i> (40%), <i>Cynadon dactylon</i> (20%)
NxaDr2	100	<i>Imperata cylindrica</i> (99%)
NxaWet1	90	<i>Imperata cylindrica</i> (60%), <i>Panicum repens</i> (25%)
NxaWet2	70	<i>Imperata cylindrica</i> (20%), <i>Panicum repens</i> (40%), <i>Fuirena pubescens</i> (10%)
NxaWet3	90	<i>Imperata cylindrica</i> (80%), <i>Panicum repens</i> (5%), <i>Cyperus longus</i> (5%)
NxaWet4	95	<i>Miscanthus junceus</i> (90%), <i>Schoenoplectus corymbosus</i> (5%)
NxaWet5	90	<i>Oxycaryum cubense</i> (85%), <i>Vossia cuspidate</i> (5%), <i>Oryza longistaminata</i> (5%)
NxaWet6	70	<i>Schoenoplectus corymbosus</i> (55%), <i>Drascenia sp</i> (10%), <i>Eleocharis dulcis</i> (5%)
NxaWet6b	100	<i>Cyperus papyrus</i> (100%)
GumDr1	40	<i>Sporobolus spicatus</i> (40%)
GumDr2	30	<i>Sporobolus spicatus</i> (15%), <i>Panicum repens</i> (10%), <i>Gis sp</i> (5%)
GumDr3	15	<i>Sporobolus spicatus</i> (15%)
GumDr4	20	<i>Cynadon dactylon</i> (15%), <i>Sporobolus spicatus</i> (5%)
GumWet1	40	<i>Cyperus dives</i> (20%), <i>Leersia hexandra</i> (10%), <i>Eleocharis dulcis</i> (5%), <i>Oryza longistaminata</i> (5%)
GumWet2	55	<i>Cyperus dives</i> (15%), <i>Schoenoplectus corymbosus</i> (15%), <i>Nymphaea nouchali</i> (10%), <i>Phragmites australis</i> (5%), <i>Leersia hexandra</i> (5%), <i>Eleocharis dulcis</i> (5%)
GumWet3	45	<i>Eleocharis dulcis</i> (35%), <i>Nymphaea nouchali</i> (10%)
GumWet4	35	<i>Cyperus papyrus</i> (25%), <i>Eleocharis dulcis</i> (10%)

418

420 Figure legends

421 Figure 1: Map of the Okavango Delta with location of sample stations and gradients, and the flooding
422 regime.

423

424 Figure 2. Vegetation BSi content (top panels) and sediment BSi content (lower panels, for top 5 cm of
425 the sediment profile) in Guma (left) and Nxaraga (right), expressed as Si per m². Sediment samples
426 are pooled samples of 3 cores per location per depth. Right of the line are the floodplain sites, to the
427 left island sites. The line itself indicates the last island site. Note the different scale of the vegetation
428 BSi axis for both sampling sites (top panels).

429

430 Figure 3: Sediment BSi in the Guma and Nxaraga sampling gradient, expressed as weight percent in
431 percent BSi per sediment dry mass. The islands sites are in the top panels (GumDr and NxaDry), the
432 wetland floodplain sites are in the lower panels (GumWet and NxaWet).

433 Figure 4. ASi in the deep cores from Nxaraga (weight percent in percent ASi per sediment dry mass),
434 in sample sites from the center of the island, through intermediate samplings and the riparian forest
435 to the floodplain. The exact location of the deep cores can be found in Fig. 1 (Deep 1-6). We have
436 specifically indicated the island center core, the riparian forest core and the floodplain core, as they
437 are specifically referred to in the results section.

438 Figure 5. Conceptual figure of Si cycling in permanent and seasonal swamps. While temporary BSi
439 storage is higher in the permanent swamps, recycling to the water column here is near complete. In
440 contrast, floodplain storage is low in the seasonal swamps, and a strong unidirectional Si transfer to
441 the islands dominates recycling to the water column.

442 References

443

444 Alexandre A, Meunier J-D, Colin F, Koud J-M (1997) Plant impact on the biogeochemical cycle of
445 silicon and related weathering processes. *Geochimica et Cosmochimica Acta* 61: 677-682.

446 Barao L, Clymans W, Vandevenne FI, Meire P, Conley DJ, Struyf E (2014) Pedogenic and biogenic
447 alkaline extracted Si distributions along a temperate land-use gradient. *European Journal of Soil*
448 *Science*, in press.

449 Bauer P, Thabeng G, Stauffer F, Kinzelbach W (2004) Estimation of the evapotranspiration rate from
450 diurnal groundwater level fluctuations in the Okavango Delta, Botswana. *Journal of Hydrology* 288:
451 344-355.

452 Bauer P, Supper R, Zimmermann S, Kinzelbach W (2006) Geoelectrical imaging of groundwater
453 salinization in the Okavango Delta, Botswana. *Journal of Applied Geophysics* 60: 126-141.

454 Bernal B & Mitsch W (2013) Carbon sequestration in freshwater wetlands in Costa Rica and
455 Botswana. *Biogeochemistry* 115: 77-93.

456 Blecker SW, McCulley RL, Chadwick OA & Kelly EF (2006) Biologic cycling of silica across a grassland
457 bioclimate sequence. *Global Biogeochemical Cycles* 20: GB3023.

458 Carey JC & Fulweiler RW (2012) The Terrestrial Silica Pump. *PLoS ONE* 7: e52932.

459 Carey JC & Fulweiler RW (2013) Nitrogen enrichment increases net silica accumulation in a
460 temperate salt marsh. *Limnology & Oceanography* 58(1): 99–111

461 Carey JC & Fulweiler RW (2014) Silica uptake by *Spartina* – evidence of multiple modes of
462 accumulation from salt marshes around the world. *Frontiers in Plant Science*: 5.

463 Cary L, Alexandre A, Meunier J-D, Boeglin J-L, Braun J-J (2005) Contribution of phytoliths to the
464 suspended load of biogenic silica in the Nyong basin rivers (Cameroon). *Biogeochemistry* 74: 101-
465 114.

466 Clymans, W, Struyf E, Govers G, Vandevenne F, Conley, DJ (2011) Anthropogenic impact on
467 amorphous silica pools in temperate soils. *Biogeosciences* 8: 2281-2293, doi:10.5194/bg-8-2281-2011

468 Conley DJ (2002) Terrestrial ecosystems and the global biogeochemical silica cycle. *Global*
469 *Biogeochemical Cycles* 16: 1121.

470 Cooke J & Leishman MR (2011) Is plant ecology more siliceous than we realise? *Trends in Plant*
471 *Science* 16: 61-68.

472 Davidson TA, Mackay AW, Wolski P, Mazebedi R, Murray-Hudson M & Todd M (2012). Seasonal and
473 spatial hydrological variability drives aquatic biodiversity in a flood-pulsed, sub-tropical wetland.
474 *Freshwater Biology* 57: 1253-1265.

475 Demaster DJ (1981) The Supply and Accumulation of Silica in the Marine-Environment. *Geochimica Et*
476 *Cosmochimica Acta* 45: 1715-1732.

477 Derry LA, Kurtz AC, Ziegler K & Chadwick OA (2005) Biological control of terrestrial silica cycling and
478 export fluxes to watersheds. *Nature* 433: 728-731.

479 Ding TP, Zhou JX, Wan DF, Chen ZY, Wang CY & Zhang F (2008) Silicon isotope fractionation in
480 bamboo and its significance to the biogeochemical cycle of silicon. *Geochimica Et Cosmochimica Acta*
481 72: 1381-1395.

482 Frings P, Clymans W, Jeppesen E, Lauridsen T, Struyf E & Conley DJ (2014) Lack of steady-state in the
483 global biogeochemical Si cycle: emerging evidence from lake Si sequestration. *Biogeochemistry* 117,
484 255-277.

485 Gumbricht T, McCarthy J & McCarthy TS (2004) Channels, wetlands and islands in the Okavango
486 Delta, Botswana, and their relation to hydrological and sedimentological processes. *Earth Surface*
487 *Processes and Landforms* 29: 15-29.

488 Hamilton S (2010) Biogeochemical implications of climate change for tropical rivers and floodplains.
489 *Hydrobiologia* 657: 19-35.

490 Hilley GE & Porder S (2008) A framework for predicting global silicate weathering and CO₂ drawdown
491 rates over geologic time-scales. *Proceedings of the National Academy of Sciences of the United*
492 *States of America* 105: 16855-16859.

493 Jennerjahn T C, Knoppers BA, de Souza WFL, Brunskill GJ, Silva EIL, Adi S (2006), Factors controlling
494 dissolved silica in tropical rivers. In *The Silicon Cycle* Ittekkot V et al. (eds.), pp. 29–51, Island
495 Press, Washington, D. C.

496 Mackay AW, Davidson T, Wolski P, Woodward S, Mazebedi R, Masamba WRL & Todd M (2012)
497 Diatom sensitivity to hydrological and nutrient variability in a subtropical, flood-pulse wetland.
498 *Ecohydrology* 5: 491-502.

499 McCarthy JM, Gumbricht T, McCarthy T, Frost P, Wessels K & Seidel F (2003) Flooding Patterns of the
500 Okavango Wetland in Botswana between 1972 and 2000. *AMBIO: A Journal of the Human*
501 *Environment* 32: 453-457.

502 McCarthy TS, McIver JR, Cairncross B, Ellery WN & Ellery K (1989) The Inorganic-Chemistry of Peat
503 from the Maunachira Channel-Swamp System, Okavango Delta, Botswana. *Geochimica Et*
504 *Cosmochimica Acta* 53: 1077-1089.

505 McCarthy TS, Ellery WN & Dangerfield JM (1998) The role of biota in the initiation and growth of
506 islands on the floodplain of the Okavango alluvial fan, Botswana. *Earth Surface Processes and*
507 *Landforms* 23: 291-316.

508 McCarthy TS, Humphries MS, Mahomed I, Le Roux P & Verhagen BT (2012) Island forming processes
509 in the Okavango Delta, Botswana. *Geomorphology* 179: 249-257.

510 Meunier JD, Keller C, Guntzer F, Riotte J, Braun JJ & Anupama K (2014) Assessment of the 1% Na₂CO₃
511 technique to quantify the phytolith pool. *Geoderma* 216: 30-35.

512 McKeague JA and Cline MG (1963) Silica in soil solutions: II. The adsorption of monosilicic acid by soil
513 and by other substances. *Canadian Journal of Soil Science* 43: 83-96.

514 Meunier JD, Keller C, Guntzer F, Riotte J, Braun JJ & Anupama K (2014) Assessment of the 1% Na₂CO₃
515 technique to quantify the phytolith pool. *Geoderma* 216: 30-35.

516 Mitsch W, Bernal B, Nahlik A, Mander Ü, Zhang L, Anderson C, Jørgensen S & Brix H (2013) Wetlands,
517 carbon, and climate change. *Landscape Ecology* 28: 583-597.

518 Müller F, Struyf E, Wanner A, Hartmann J, Jensen K (2013) A comprehensive study of silica pools and
519 fluxes in Wadden Sea salt marshes. *Estuaries & Coasts* 36: 1150-1164.

520 Ramberg L & Wolski P (2008) Growing islands and sinking solutes: processes maintaining the
521 endorheic Okavango Delta as a freshwater system. *Plant Ecology* 196: 215-231.

522 Saccone L, Conley DJ, Koning E, Sauer D, Sommer M, Kaczorek D, Blecker SW & Kelly EF (2007)
523 Assessing the extraction and quantification of amorphous silica in soils of forest and grassland
524 ecosystems. *European Journal of Soil Science* 58: 1446-1459.

525 Sawula G & Martins E (1991) Major ion chemistry of the lower Boro River, Okavango Delta,
526 Botswana. *Freshwater Biology* 26: 481-493.

527 Schaller J, Struyf E (2013) Silicon controls microbial decay and nutrient release of grass litter during
528 aquatic decomposition. *Hydrobiologia* 709: 201-212.

529 Schoelynck J, Bal K, Backx H, Okruszko T, Meire P & Struyf E (2010) Silica uptake in aquatic and
530 wetland macrophytes: a strategic choice between silica, lignin and cellulose? *New Phytologist* 186:
531 385-391.

532 Schoelynck J, Müller F, Vandevenne F, Bal K, Barão L, Smis A, Opdekamp W, Meire P, Struyf E, (2014)
533 Silicon-vegetation interaction in multiple ecosystems: a review. *Journal of Vegetation Science* 25:
534 301-313.

535 Struyf E, Van Damme S, Gribsholt B, Middelburg JJ & Meire P (2005) Biogenic silica in freshwater
536 marsh sediments and vegetation. *Marine Ecology Progress Series* 303: 51-60.

537 Struyf E, Dausse A, Van Damme S, Bal K, Gribsholt B, Boschker HTS, Middelburg JJ & Meire P (2006)
538 Tidal marshes and biogenic silica recycling at the land-sea interface. *Limnology & Oceanography*
539 51(2): 838-846

540 Struyf E, Van Damme S, Gribsholt B, Bal K, Beauchard O, Middelburg JJ & Meire P (2007) *Phragmites*
541 *australis* and silica cycling in tidal wetlands. *Aquatic Botany* 87: 134-140.

542 Struyf E, Conley DJ (2009) Silica: an essential nutrient in wetland biogeochemistry. *Frontiers in*
543 *Ecology and Environment* 7(2): 88-94.

544 Struyf E, Opdekamp W, Backx H, Jacobs S, Conley DJ & Meire P (2009) Vegetation and proximity to
545 the river control amorphous Si storage in a riparian wetland (Bierbza National Park, Poland).
546 *Biogeosciences* 6: 623-631.

547 Struyf E, Mörth M, Humborg C & Conley DJ (2010) An enormous amorphous silica pool in boreal
548 wetlands. *Journal of Geophysical Research* 115: G04008.

549 Struyf E & Conley DJ (2012) Emerging understanding of the ecosystem silica filter. *Biogeochemistry*
550 107: 9-18.

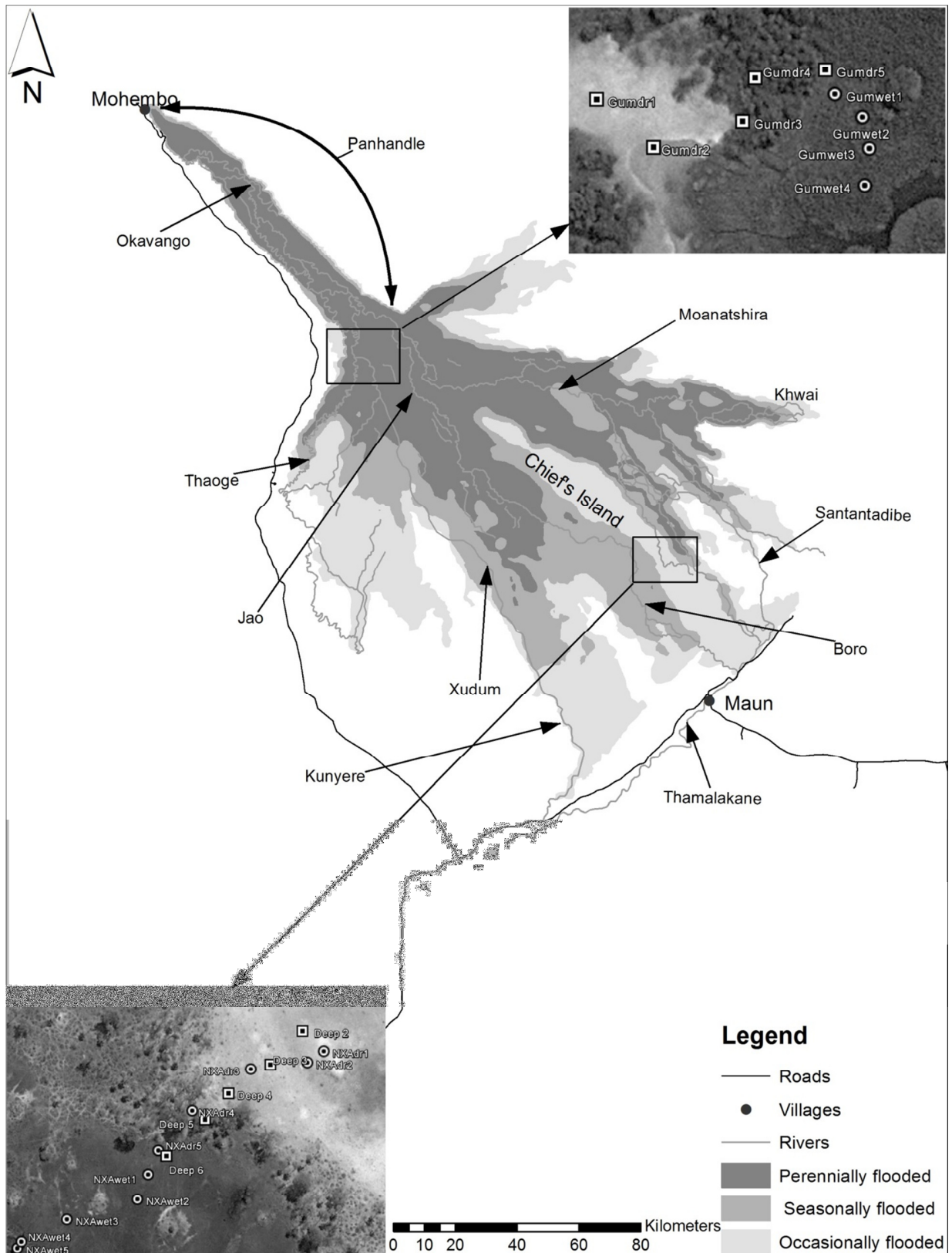
551 Tréguer PJ & De La Rocha CL (2013) The World Ocean Silica Cycle. *Annual Review of Marine Science*
552 5: 477-501.

553 Wolski P, Savenije HHG, Murray-Hudson M & Gumbricht T (2006) Modelling of the flooding in the
554 Okavango Delta, Botswana, using a hybrid reservoir-GIS model. *Journal of Hydrology* 331: 58-72.

555 Wolski P, Stone D, Tadross M, Wehner M & Hewitson B (2014) Attribution of floods in the Okavango
556 basin, Southern Africa. *Journal of Hydrology* 511: 350-358.

557 Zimmermann S, Bauer P, Held R, Kinzelbach W, Walther JH (2006) Salt transport on islands in the
558 Okavango Delta: Numerical investigations. *Advances in Water Resources* 29: 11-29.

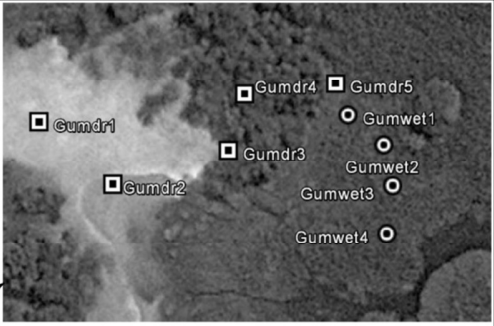
559



Mohembo

Panhandle

Okavango



Moanatshira

Khwai

Chief's Island

Santantadibe

Thaoge

Jao

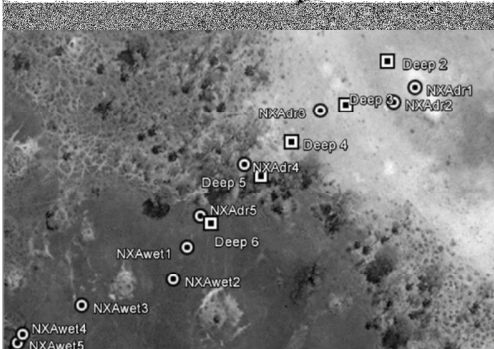
Boro

Xudum

Maun

Kunyere

Thamalakane



Legend

- Roads
- Villages
- - - Rivers
- Perennially flooded
- Seasonally flooded
- Occasionally flooded

0 10 20 40 60 80 Kilometers

